Metal-insulator transition in the ground state of the three-band Hubbard model at half filling

Ettore Vitali,[1,2] Hao Shi,[3] Adam Chiciak,[2] and Shiwei Zhang[2,3]
[1]*Department of Physics, California State University Fresno, Fresno, California 93740, USA*
[2]*Department of Physics, The College of William and Mary, Williamsburg, Virginia 23187, USA*
[3]*Center for Computational Quantum Physics, Flatiron Institute, 162 5th Avenue, New York, New York 10010, USA*

(Received 16 July 2018; revised manuscript received 25 March 2019; published 12 April 2019)

The three-band Hubbard model is a fundamental model for understanding properties of the copper-oxygen planes in cuprate superconductors. We use cutting-edge auxiliary-field quantum Monte Carlo (AFQMC) methods to investigate ground state properties of the model in the parent compound. Large supercells combined with twist averaged boundary conditions are employed to reliably reach the thermodynamic limit. Benchmark quality results are obtained on the magnetic correlations and charge gap. A key parameter of this model is the charge-transfer energy Δ between the oxygen p and the copper d orbitals, which appears to vary significantly across different families of cuprates and whose *ab initio* determination is subtle. We show that the system undergoes a quantum phase transition from an antiferromagnetic insulator to a paramagnetic metal as Δ is lowered to 3 eV.

DOI: 10.1103/PhysRevB.99.165116

I. INTRODUCTION

It is widely believed that the physical mechanism underlying high-temperature superconductivity in the cuprate materials lies in the quasi-two-dimensional physics of the CuO_2 planes. A significant amount of the theoretical studies of such planes (see, e.g., Refs. [1,2] for some recent reviews) have relied on the celebrated Hubbard Hamiltonian [3,4], which is a minimal low-energy effective model that assumes the explicit contribution of the oxygen degrees of freedom can be neglected. Although impressively accurate results [5] have been obtained on the one-band Hubbard model and very interesting magnetic and charge orders have emerged [6,7] which are relevant to some important experimental results, it is still unclear whether the model can support long-range superconducting correlations in the ground state. While this answer in the one-band Hubbard model (or perhaps the closely related t-J model which could contain different physics [8–11]) is clearly important and of fundamental value, it is timely, based on current results, to revisit what the effect of additional realism is and what might be a more accurate minimal model of the CuO_2 plane.

With the advent of modern computing platforms and progress in the development of numerical methods, it is now possible to reach beyond the one-band model in favor of the more realistic, although still minimal, three-band Hubbard model, also called the Emery model [12], and obtain computational results of high accuracy and sufficiently close to the thermodynamic limit. In this work, we perform an extensive study of the ground state of this model for the parent compounds, employing the cutting-edge constrained-path auxiliary-field quantum Monte Carlo (CP-AFQMC) method [13,14], together with recently developed self-consistency loops [15] to systematically improve the approximation needed because of the fermion sign problem. The method maintains polynomial computational complexity, and we study large supercells under twisted boundary conditions to determine properties at the thermodynamic limit.

The three-band Hubbard model includes the Cu $3d_{x^2-y^2}$ orbital together with the O $2p_x$ and $2p_y$ orbitals. Most parameter values of the Hamiltonian can be derived by *ab initio* methods for real materials with reasonable reliability. Among these the charge transfer energy Δ has been found to vary substantially across different families of cuprate materials, as illustrated in Fig. 1. Furthermore, it is known that *ab initio* computations to determine its value often have difficulties [16,17]. This parameter is important because it directly controls the hole density on the Cu sites, which is seen to be anticorrelated with the superconducting critical temperature [18–21]. Here we investigate the ground-state properties of the parent compound as a function of Δ, using state-of-the-art quantum Monte Carlo calculations. The calculations reach an accuracy and predictive power well beyond previously possible, and benchmark quality results are obtained on the magnetic correlations and charge gaps in the ground state. We find that a quantum phase transition occurs at $\Delta \sim 3$ eV between a paramagnetic metal and an antiferromagnetic insulator.

II. BACKGROUND AND METHODOLOGY

The Hamiltonian of the three-band Hubbard model is

$$\begin{aligned}\hat{H} = {} & \varepsilon_d \sum_{i,\sigma} \hat{d}^\dagger_{i,\sigma}\hat{d}_{i,\sigma} + \varepsilon_p \sum_{j,\sigma} \hat{p}^\dagger_{j,\sigma}\hat{p}_{j,\sigma} \\ & + \sum_{\langle i,j\rangle,\sigma} t^{ij}_{pd}(\hat{d}^\dagger_{i,\sigma}\hat{p}_{j,\sigma} + \text{H.c.}) + \sum_{\langle j,k\rangle,\sigma} t^{jk}_{pp}(\hat{p}^\dagger_{j,\sigma}\hat{p}_{k,\sigma} + \text{H.c.}) \\ & + U_d \sum_i \hat{d}^\dagger_{i,\uparrow}\hat{d}_{i,\uparrow}\hat{d}^\dagger_{i,\downarrow}\hat{d}_{i,\downarrow} + U_p \sum_j \hat{p}^\dagger_{j,\uparrow}\hat{p}_{j,\uparrow}\hat{p}^\dagger_{j,\downarrow}\hat{p}_{j,\downarrow}.\end{aligned} \tag{1}$$

A pictorial representation of the CuO_2 plane is given in Fig. 1. We will measure lengths in units of the distance between nearest neighbors Cu sites. In Eq. (1), the label i runs over the sites $\mathbf{r}_{\text{Cu}}$ of a square lattice $\mathbb{Z}^2$ of Cu atoms. The labels j and k run over the positions of the O atoms, shifted with respect to

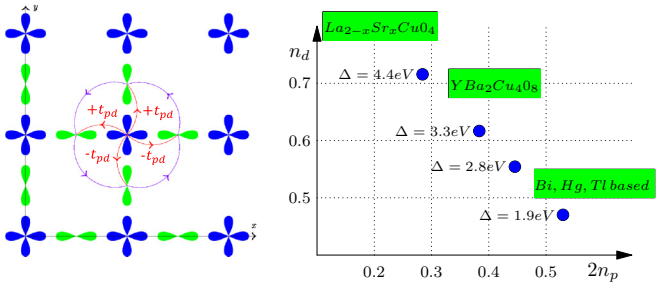

FIG. 1. (Left) Schematic view of the CuO_2 plane of the cuprates. Cu $3d_{x^2-y^2}$ orbitals are represented in blue, and O $2p_x$ and $2p_y$ orbitals in green. The curve connectors represent the hopping, and the labels define the sign rule. (Right) Density of holes around the d and the p sites ($n_d + 2n_p = 1$) as a function of Δ. Results computed from AFQMC are given by blue circles. The green boxes indicate the typical values observed (or extrapolated from) in families of cuprate materials [19,20]: $n_d \simeq 0.83$ for La-based, $\simeq$0.7 for Y-based, and $\simeq$0.5 for Bi- and Hg-based cuprates.

the Cu sites, $\mathbf{r}_O = \mathbf{r}_{Cu} + 0.5\,\mathbf{l}$, where the unit vector $\mathbf{l}$ is $\hat{x}$ for the $2p_x$ and $\hat{y}$ for the $2p_y$ orbitals. The model is formulated in terms of holes: e.g., $\hat{d}^\dagger_{i,\sigma}$ creates a hole on the $3d_{x^2-y^2}$ orbital at site i with spin $\sigma = \uparrow$ or $\downarrow$. The first two terms define a charge transfer energy $\Delta \equiv \varepsilon_p - \varepsilon_d$, representing the energy needed for a hole to move from a $3d_{x^2-y^2}$ to a p orbital. The second two terms describe hopping between orbitals; the hopping amplitudes $|t^{ij}_{pd}| = t_{pd}$ and $|t^{jk}_{pp}| = t_{pp}$, with sign convention as illustrated in Fig. 1. Finally, the last two terms represent the on-site repulsion energies, double-occupancy penalties, as in the Hubbard model.

At half filling, when there are equal numbers of holes and Cu atoms in the lattice, the model describes the parent compound, which is known from experiments to be an insulating antiferromagnet. Adding (removing) holes corresponds to hole (electron) doping. Experimentally, with hole doping, the magnetic order rapidly melts and superconductivity arises which competes or cooperates with several forms of spin and charge order. Naturally, before addressing the topic of superconductivity in the underdoped regime, it is important to determine the behavior of the model at half filling.

The Emery model has been studied using several different numerical approaches: exact diagonalization [22,23], cluster perturbation theory [24], generalized random phase approximation [25], quantum Monte Carlo [26–28], density matrix renormalization group [29], and dynamical mean field theory or its cluster generalizations [30]. Here we use the CP-AFQMC method [13,14], which controls the fermion sign problem with a CP approximation that can be systematically improved via a self-consistency procedure [15]. This approach, which has demonstrated consistently high accuracy [5,6], represents the state-of-the-art many-body computational technology for such a system. Our results provide a detailed characterization of the ground state properties and reference data on this model. Our calculations establish unambiguously the existence of a metal-insulator transition as a function of the charge transfer energy.

Most parameters in the Hamiltonian in Eq. (1) have "canonical" values obtained from band structure or other calculations. We will use a set of parameters obtained for $La_2Cu\,O_4$, the parent compound of the lanthanum family of cuprates: $\varepsilon_p = -3.2$, $\varepsilon_d = -7.6$, $t_{pd} = 1.2$, $t_{pp} = 0.7$, $U_p = 2$, and $U_d = 8.4$ (all in units of eV). The charge transfer energy, however, entails more uncertainty. The set above gives $\Delta = 4.4$ eV, but theoretical arguments based on double counting corrections [16] would imply a significant reduction to this value. Within generalized Hartree-Fock (GHF), a strong dependence of the ground-state magnetic properties on Δ is seen [31]. Moreover, in real materials, significant variations have been observed in Δ, which can be broadly tuned through chemical substitution and strain [32]. Recent nuclear magnetic resonance experiments [20] have shown that, as a result, the hole densities on Cu vary, which in turn affects the critical superconducting transition temperature. In this study, we scan the value of the charge transfer energy from $\Delta = 4.4$ to 1.5 eV.

We study systems of N holes in an $M = L \times L$ lattice, i.e., a supercell of Cu_MO_{2M}. Calculations are performed on systems as large as $L = 12$, containing 432 atoms in the supercell. Special care was taken in the extrapolations to the thermodynamic limit. Several checks were carried out, with rectangular supercell shapes and with different boundary conditions (periodic and twisted). Additionally, calculations with a pinning field to break translational symmetry were also done in order to verify the robustness of the long-range order.

To compute properties of the ground state $|\Psi_0\rangle$ of the model, we use the CP-AFQMC method, which relies on a projection from an initial or trial wave function:

$$|\Psi_0\rangle \propto \lim_{\beta\to+\infty} \exp(-\beta(\hat{H} - E_0))\,|\psi_T\rangle\,, \tag{2}$$

where E_0 is the ground-state energy which is estimated adaptively in the process. The method realizes the projection with a stochastic dynamics in the manifold of wave functions of independent particles embedded in random external auxiliary fields. The trial wave function $|\psi_T\rangle$ plays an important role in the methodology. It is used to impose an approximate constraint to the random walk, in order to control the fermion sign problem and keep the computational complexity at $\mathcal{O}(N^3)$. To maximize the accuracy and predictive power of the approach, we use a self-consistent scheme [7] to encode the information from the CP-AFQMC as feedback in generating a new $|\psi_T\rangle$. We measure the order parameter of a broken-symmetry solution of the many-body Hamiltonian with pinning fields. A trial wave function is generated using GHF [31]. The CP-AFQMC calculation with this $|\psi_T\rangle$ obtains the density matrix, which is then fed into another GHF calculation with renormalized Hamiltonian parameters (Δ and U_d) that are tuned to minimize the difference between the density matrix it produces and that from the CP-AFQMC. The new GHF solution is then used in a new CP-AFQMC calculation and the process is iterated until convergence. This approach has been shown to give very accurate results in a variety of correlated systems including the one-band Hubbard model [5–7].

III. RESULTS

In Table I we show the computed ground-state energy per unit cell as a function of Δ. The results are obtained as an

TABLE I. Energy per unit cell as a function of the charge-transfer energy. The values are based on calculations in 12×12 supercells with twist averaging.

Δ (eV)	1.9	2.8	3	3.3	4.4
E/M (eV)	−10.082(8)	−9.639(2)	−9.556(2)	−9.437(2)	−9.071(6)

average over twist angles in the boundary conditions. The complex phase arising from the twist boundary condition is handled straightforwardly [33]. The computed energy is robust with respect to $|\psi_T\rangle$; the mixed estimate [34] is used and no self-consistency iteration is necessary for these results. The system is large enough such that any residual finite-size effects are expected to be comparable to the statistical error bar. This was estimated by select calculations with even larger supercell sizes. These results should provide a valuable benchmark in future studies of the Emery model.

Magnetic properties are presented in Fig. 2. We measure spin correlation functions of the form $C_S(\mathbf{r}) = \langle \hat{\mathbf{S}}(\mathbf{0}) \cdot \hat{\mathbf{S}}(\mathbf{r}) \rangle$, where the spin operator is defined as usual: $\hat{\mathbf{S}}(\mathbf{r}) = \frac{1}{2} \sum_{\sigma,\sigma'} \boldsymbol{\sigma}_{\sigma,\sigma'} \hat{d}^\dagger_{i,\sigma} \hat{d}_{i,\sigma'}$, with $\boldsymbol{\sigma}_{\sigma,\sigma'}$ denoting elements of the Pauli matrices, and the expectation $\langle \cdots \rangle$ is with respect to the many-body ground state $|\Psi_0\rangle$, which requires back propagation [34]. The upper panel is a color plot of $C_S(\mathbf{r})$ for $\Delta = 4.4$ eV. The correlation function is seen to vanish on the p sites, where no magnetism is observed. On the other hand, long-range antiferromagnetic (AFM) order is evident on the Cu atoms. The lower panel shows the order parameter $|S(\mathbf{r})| \equiv |C_S(\mathbf{r})|^{1/2}$ for $|\mathbf{r}| \geqslant 3$ as the values of the charge transfer energy Δ is varied. A nonzero AFM order parameter is seen for $\Delta \geqslant 3$ eV, which becomes compatible with zero for $\Delta \leqslant 2.8$ eV, signaling the presence of a phase transition at $\Delta \sim 3$ eV. The asymptotic value of the AFM order parameter (taken as an average over $|\mathbf{r}| \geqslant 3$) is plotted as a function of Δ in the upper panel of Fig. 3.

To further examine the properties of the system as Δ becomes smaller, we probe the electrical conductivity in the

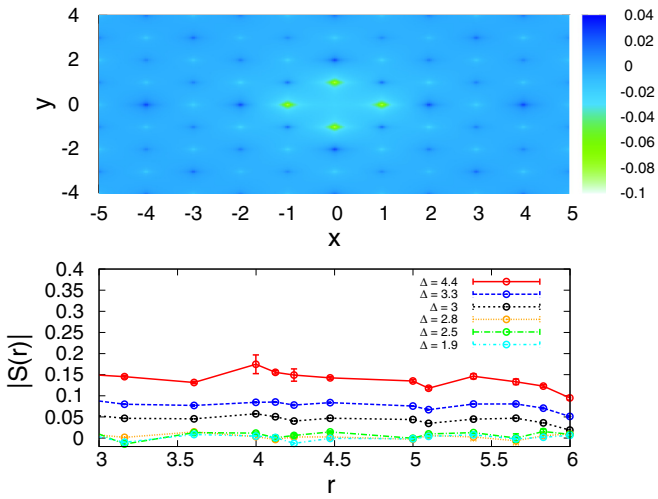

FIG. 2. Computed ground-state magnetic properties. The upper panel shows a color plot of the spin correlation function at $\Delta = 4.4$ eV for a 12×12 supercell. The lower panel shows the order parameter at asymptotic distances for a sequence of Δ values.

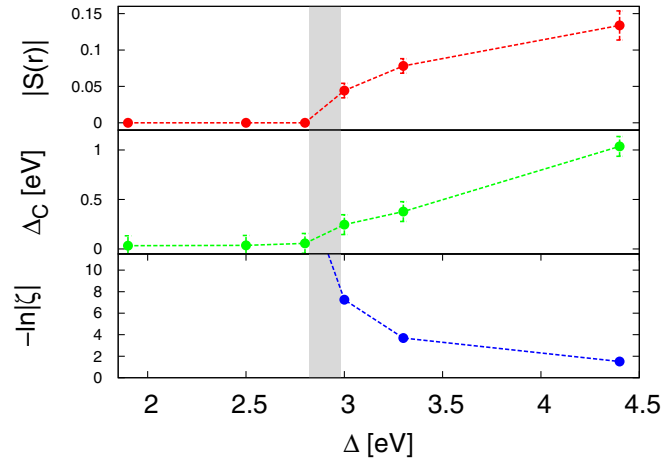

FIG. 3. Metal-insulator transition as a function of the charge transfer energy Δ. Three different signatures are computed: antiferromagnetic order parameter $|S(\vec{r})|$ (upper panel), charge gap Δ_C as defined in Eq. (4) (middle panel), logarithm of the localization measure in Eq. (3) (lower panel). The values of $-ln|\zeta|$ for $\Delta < 3$ eV are compatible with $+\infty$. The shaded area indicates the phase transition region.

ground state. Following Resta and Sorella [35], we compute the complex-valued localization measure of the holes:

$$\zeta = \langle \Psi_0 | e^{i \frac{2\pi}{L} \hat{X}} | \Psi_0 \rangle , \tag{3}$$

where, without loss of generality, we have chosen the quantum mechanical position operator $\hat{X} = \hat{x}_1 + \cdots + \hat{x}_N$ to be along the x direction. The quantity ζ, which is related to the quantum metric tensor, has a geometrical interpretation and plays an important role in the modern theory of electric polarization. A nonzero value of $|\zeta|$ for a large number of holes implies a localized many-body ground state and thus an insulator, while a vanishing $|\zeta|$ indicates a delocalized ground state and a conductor. The dependence of $|\zeta|$ on Δ is shown in the lower panel of Fig. 3. The result is consistent with a phase transition from an antiferromagnetic, insulating ground state at $\Delta \geqslant 3$ eV to a nonmagnetic metal at smaller values of the charge-transfer energy. To our knowledge, our calculations here represent one of the first computations of Eq. (3) with an advanced many-body method in a strongly correlated physical system whose ground state is unknown.

We also compute the charge gap of the system

$$\Delta_C = E(N+1) + E(N-1) - 2E(N) , \tag{4}$$

where $E(N)$ is the ground-state energy at half filling, while $E(N \pm 1)$ denotes the ground-state energies of the system with one hole added/removed. In Ref. [36] Eq. (4) was compared with the standard definition in terms of Green functions in the Hubbard model, and it was shown numerically that they lead to identical gaps. (For a superconducting system, this definition would give the pairing gap. An alternative to Eq. (4) would be to compute the two-particle gap [37,38], where $N \pm 1$ is replaced by $N \pm 2$. The latter can be an important property to address in future studies, in particular when transitions from insulators to superconductors are expected.) The gap is a central quantity which can be directly measured

in photoemission spectroscopy experiments. Its calculation can be challenging because of finite-size and shell effects arising from the noninteracting part of the Hamiltonian. We use a scheme [36] utilizing twist averaging to accelerate convergence to the thermodynamic limit. We find that the dependence on the twist parameter is rather weak here, allowing converged results with only a handful of twist angles in our measurement. A subtlety also exists in the choice of trial wave functions for the $(N \pm 1)$ systems. As mentioned before, we build $|\psi_T\rangle$ through a self-consistent procedure providing a GHF Hamiltonian with renormalized parameters. By using the same mean-field Hamiltonian to generate the $|\psi_T\rangle$'s for $(N-1)$, N, and $(N+1)$ systems, we see better error cancellation in tests on smaller systems and adopt this procedure in the calculation of gaps. The result is shown in the middle panel of Fig. 3. A finite charge gap is seen for $\Delta \geqslant 3$ eV, which vanishes at smaller Δ. The experimental gap for La_2CuO_4 is 1.5–2 eV [39–42], while, for Bi-based materials, a value of 1–1.5 eV [18] is found. The experimental trend is consistent with our data, showing the gap decreasing as Δ, and thus n_d, decreases. However, the experimental values are higher than our corresponding results, which is likely due to the much simplified nature of the model and the uncertainty in the parameter choices.

The three independent signatures shown in Fig. 3, the AFM correlation function, the localization measure, and the charge gap, all point to a consistent picture of the ground state, with a phase transition from an insulating to a metallic ground state at a charge transfer energy of $\Delta \sim 3$ eV.

We also investigate the charge density and correlation functions and the d-wave pairing correlations. In the right panel of Fig. 1, the computed hole densities on the Cu and O sites are shown for four different Δ values spanning the transition. Similar to the spin correlation function, we define the charge correlation: $C_C(\mathbf{r}) = \langle \hat{n}(\mathbf{0})\hat{n}(\mathbf{r})\rangle / \langle \hat{n}(\mathbf{0})\rangle \langle \hat{n}(\mathbf{r})\rangle$, where the density operator is, for Cu sites, $\hat{n}(\mathbf{r}) = \sum_\sigma \hat{d}^\dagger_{i,\sigma}\hat{d}^\dagger_{i,\sigma}$, and similarly for the O sites. The pairing correlation function is defined as: $C_\Delta(\mathbf{r}) = \langle \hat{\Delta}(\mathbf{0})\hat{\Delta}^\dagger(\mathbf{r})\rangle$ where the d-wave pairing operator $\hat{\Delta}(\mathbf{r})$ is defined as in Ref. [27]. The results are shown in Fig. 4.

It is clear that there is no charge and pairing long-range order in the system at half filling, as expected. The density correlation function displays only a very short-range repulsive exchange-correlation hole. As Δ is increased, the correlation between nearest-neighbor d and p orbitals decreases while the nearest-neighbor d-d correlation increases, another clear signature of AFM. For the smallest Δ, the nearest neighbors d-p correlation is almost identical to the noninteracting result, while the nearest neighbor d-d is slightly higher.

Observing the distance dependence of the pairing correlation, we see that, at very short range, the correlations increase with Δ, likely due to the tendency for antiferromagnetic correlations. At longer range, the opposite tendency is seen, with the pairing correlations increasing as Δ is decreased. This result is consistent with the experimental evidence [18–21] that the charge-transfer energy is anticorrelated with the superconducting critical temperature. It suggests a picture of local tendency towards AFM order which allows the system to build d-wave pairs that become more correlated once the holes become more delocalized.

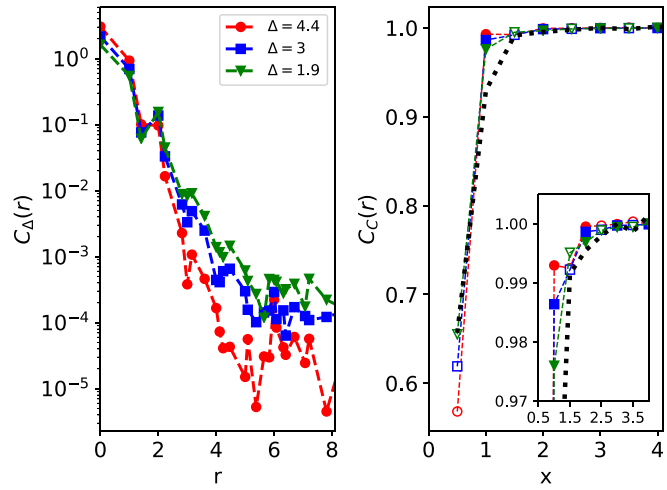

FIG. 4. (Left panel) Distance dependence of the d-wave pairing correlation function $C_\Delta(\mathbf{r})$ for a few values of the charge transfer energy. (Right panel) Density correlation function $C_C(\mathbf{r})$ plotted along the Cu-O bond. We denote x the coordinate along the bond, as in Fig. 1. We use open symbols for correlations involving one d orbital and one p_x, while solid symbols indicate d-d correlations. The noninteracting result, which does not depend on Δ, is also shown (black dotted line) for reference. The inset is a zoom in, for $x > 0.5$.

IV. DISCUSSION AND SUMMARY

Before drawing our conclusions, we provide a brief discussion of the results in the broader context. As we have mentioned, there are a number of studies of the Emery model already in the literature. At present no numerical methods can reach the thermodynamic limit free of any bias. We have emphasized that the CP-AFQMC approach is not exact because of the control on the sign problem. We should also emphasize that it has consistently demonstrated, via many applications and extensive collaborative benchmark projects [5,43], an outstanding balance of accuracy and the ability to scale reliably to the thermodynamic limit. The numerical results in this paper reflect a kind of state of the art, and residual effect from CP is expected to be minimal. Clearly it would be very desirable to apply a similar level of computational technologies to tackle the many remaining questions in the Emery model, including magnetic and superconducting properties upon doping. Here recent progress in computing dynamical Green functions and excitation information [36,44] can provide crucial additional capabilities.

In summary, we performed an extensive study of the ground state of the Emery model at half filling using cutting-edge AFQMC calculations. The favorable computational scaling of the algorithm allowed us to study supercells as large as 12×12 which, together with twist averaging, makes it possible to access properties at the thermodynamic limit. We investigated the role of the charge transfer energy Δ, whose value varies across different families of cuprate materials. Accurate results on the spin correlation functions, the localization or conductivity measure, and the charge gap are computed versus Δ for a set of canonical Hamiltonian parameters. Ground-state energies, charge densities and correlation functions, and pairing correlations are also determined. The tendency of d-wave pairing is seen to increase as Δ decreases. Our results establish unambiguously a quantum

phase transition in the ground state of this fundamental model connecting an antiferromagnetic insulator to a nonmagnetic metal as Δ is decreased to $\sim$3 eV.

ACKNOWLEDGMENTS

We thank the Simons Foundation and NSF (Grant No. DMR-1409510) for their support. Computing was carried out at the Extreme Science and Engineering Discovery Environment (XSEDE), which is supported by National Science Foundation Grant No. ACI-1053575, and the High Performance Computational facilities at William and Mary. The Flatiron Institute is a division of the Simons Foundation.

[1] E. Fradkin, S. A. Kivelson, and J. M. Tranquada, Rev. Mod. Phys. **87**, 457 (2015).
[2] P. A. Lee, N. Nagaosa, and X.-G. Wen, Rev. Mod. Phys. **78**, 17 (2006).
[3] J. Hubbard, Proc. R. Soc. London, Ser. A **276**, 238 (1963).
[4] M. C. Gutzwiller, Phys. Rev. Lett. **10**, 159 (1963).
[5] J. P. F. LeBlanc, A. E. Antipov, F. Becca, I. W. Bulik, G. K.-L. Chan, C.-M. Chung, Y. Deng, M. Ferrero, T. M. Henderson, C. A. Jiménez-Hoyos, E. Kozik, X.-W. Liu, A. J. Millis, N. V. Prokof'ev, M. Qin, G. E. Scuseria, H. Shi, B. V. Svistunov, L. F. Tocchio, I. S. Tupitsyn, S. R. White, S. Zhang, B.-X. Zheng, Z. Zhu, and E. Gull (Simons Collaboration on the Many-Electron Problem), Phys. Rev. X **5**, 041041 (2015).
[6] B.-X. Zheng, C.-M. Chung, P. Corboz, G. Ehlers, M.-P. Qin, R. M. Noack, H. Shi, S. R. White, S. Zhang, and G. K.-L. Chan, Science **358**, 1155 (2017).
[7] M. Qin, H. Shi, and S. Zhang, Phys. Rev. B **94**, 085103 (2016).
[8] S. Sorella, G. B. Martins, F. Becca, C. Gazza, L. Capriotti, A. Parola, and E. Dagotto, Phys. Rev. Lett. **88**, 117002 (2002).
[9] N. M. Plakida, Condens. Matter Phys. **5**, 707 (2002).
[10] S. Sachdev and R. La Placa, Phys. Rev. Lett. **111**, 027202 (2013).
[11] M. Bejas, A. Greco, and H. Yamase, Phys. Rev. B **86**, 224509 (2012).
[12] V. J. Emery, Phys. Rev. Lett. **58**, 2794 (1987).
[13] S. Zhang, J. Carlson, and J. E. Gubernatis, Phys. Rev. Lett. **74**, 3652 (1995).
[14] S. Zhang, *Auxiliary-Field Quantum Monte Carlo for Correlated Electron Systems*, Vol. 3 of *Emergent Phenomena in Correlated Matter: Modeling and Simulation*, edited by E. Pavarini, E. Koch, and U. Schollwöck (Verlag des Forschungszentrum Jülich, Jülich, 2013).
[15] M. Qin, H. Shi, and S. Zhang, Phys. Rev. B **94**, 235119 (2016).
[16] P. R. C. Kent, T. Saha-Dasgupta, O. Jepsen, O. K. Andersen, A. Macridin, T. A. Maier, M. Jarrell, and T. C. Schulthess, Phys. Rev. B **78**, 035132 (2008).
[17] M. S. Hybertsen, M. Schlüter, and N. E. Christensen, Phys. Rev. B **39**, 9028 (1989).
[18] W. Ruan, C. Hu, J. Zhao, P. Cai, Y. Peng, C. Ye, R. Yu, X. Li, Z. Hao, C. Jin, X. Zhou, Z.-Y. Weng, and Y. Wang, Sci. Bull. **61**, 1826 (2016).
[19] M. Jurkutat, D. Rybicki, O. P. Sushkov, G. V. M. Williams, A. Erb, and J. Haase, Phys. Rev. B **90**, 140504(R) (2014).
[20] D. Rybicki, M. Jurkutat, S. Reichardt, C. Kapusta, and J. Haase, Nat. Commun. **7**, 11413 (2016).
[21] C. Weber, C. Yee, K. Haule, and G. Kotilar, Europhys. Lett. **100**, 37001 (2012).
[22] C.-C. Chen, B. Moritz, F. Vernay, J. N. Hancock, S. Johnston, C. J. Jia, G. Chabot-Couture, M. Greven, I. Elfimov, G. A. Sawatzky, and T. P. Devereaux, Phys. Rev. Lett. **105**, 177401 (2010).
[23] C.-C. Chen, M. Sentef, Y. F. Kung, C. J. Jia, R. Thomale, B. Moritz, A. P. Kampf, and T. P. Devereaux, Phys. Rev. B **87**, 165144 (2013).
[24] D. Sénéchal, D. Perez, and D. Plouffe, Phys. Rev. B **66**, 075129 (2002).
[25] S. Bulut, A. P. Kampf, and W. A. Atkinson, Phys. Rev. B **92**, 195140 (2015).
[26] Y. F. Kung, C.-C. Chen, Y. Wang, E. W. Huang, E. A. Nowadnick, B. Moritz, R. T. Scalettar, S. Johnston, and T. P. Devereaux, Phys. Rev. B **93**, 155166 (2016).
[27] M. Guerrero, J. E. Gubernatis, and S. Zhang, Phys. Rev. B **57**, 11980 (1998).
[28] E. W. Huang, C. B. Mendl, S. Liu, S. Johnston, H.-C. Jiang, B. Moritz, and T. P. Devereaux, Science **358**, 1161 (2017).
[29] S. R. White and D. J. Scalapino, Phys. Rev. B **92**, 205112 (2015).
[30] A. Go and A. J. Millis, Phys. Rev. Lett. **114**, 016402 (2015).
[31] A. Chiciak, E. Vitali, H. Shi, and S. Zhang, Phys. Rev. B **97**, 235127 (2018).
[32] C.-H. Yee and G. Kotliar, Phys. Rev. B **89**, 094517 (2014).
[33] C.-C. Chang and S. Zhang, Phys. Rev. B **78**, 165101 (2008).
[34] S. Zhang, J. Carlson, and J. E. Gubernatis, Phys. Rev. B **55**, 7464 (1997).
[35] R. Resta and S. Sorella, Phys. Rev. Lett. **82**, 370 (1999).
[36] E. Vitali, H. Shi, M. Qin, and S. Zhang, Phys. Rev. B **94**, 085140 (2016).
[37] E. Berg, E. Fradkin, E.-A. Kim, S. A. Kivelson, V. Oganesyan, J. M. Tranquada, and S. C. Zhang, Phys. Rev. Lett. **99**, 127003 (2007).
[38] N. Furukawa and M. Imada, J. Phys. Soc. Jpn. **60**, 3604 (1991).
[39] Y. Tokura, S. Koshihara, T. Arima, H. Takagi, S. Ishibashi, T. Ido, and S. Uchida, Phys. Rev. B **41**, 11657 (1990).
[40] S. L. Cooper, G. A. Thomas, A. J. Millis, P. E. Sulewski, J. Orenstein, D. H. Rapkine, S.-W. Cheong, and P. L. Trevor, Phys. Rev. B **42**, 10785 (1990).
[41] S. Uchida, T. Ido, H. Takagi, T. Arima, Y. Tokura, and S. Tajima, Phys. Rev. B **43**, 7942 (1991).
[42] J. P. Falck, A. Levy, M. A. Kastner, and R. J. Birgeneau, Phys. Rev. Lett. **69**, 1109 (1992).
[43] M. Motta, D. M. Ceperley, G. K.-L. Chan, J. A. Gomez, E. Gull, S. Guo, C. A. Jiménez-Hoyos, T. N. Lan, J. Li, F. Ma, A. J. Millis, N. V. Prokof'ev, U. Ray, G. E. Scuseria, S. Sorella, E. M. Stoudenmire, Q. Sun, I. S. Tupitsyn, S. R. White, D. Zgid, and S. Zhang (Simons Collaboration on the Many-Electron Problem), Phys. Rev. X **7**, 031059 (2017).
[44] E. Vitali, H. Shi, M. Qin, and S. Zhang, Phys. Rev. A **96**, 061601(R) (2017).